

## Supporting Information

### Improved photo-redox activity of 2D $\text{Bi}_4\text{Ti}_3\text{O}_{12}$ - $\text{BiVO}_4$ - $\text{Bi}_4\text{V}_2\text{O}_{10}$ heterostructure via piezoelectric-enhanced charge transfer effect

Wuyou Wang ‡<sup>a,\*</sup>, Kai Zhu ‡<sup>a,e</sup>, Beibei Zhang <sup>a</sup>, Xiaowei Chen <sup>b</sup>, Dongqi Ma <sup>a</sup>, Xuewen Wang <sup>d</sup>, Rongbin Zhang <sup>d</sup>, Yin Liu <sup>e</sup>, Jinxin Shen <sup>a</sup>, Pengyu Dong <sup>c,\*</sup>, Xinguo Xi <sup>b,c,\*</sup>

a. School of Chemistry & Chemical Engineering, Yancheng Institute of Technology, Yancheng 224051, PR China

b. School of Materials Science and Engineering, Yancheng Institute of Technology, Yancheng 224051, PR China

c. Key Laboratory for Advanced Technology in Environmental Protection of Jiangsu Province, Yancheng Institute of Technology, Yancheng 224051, PR China

d. Key Laboratory of Jiangxi Province for Environment and Energy Catalysis, the College of Chemistry, Nanchang University, Nanchang 330031, PR China

e. School of Materials Science and Engineering, Anhui University of Science and Technology, Huainan 232001, PR China

\*Corresponding author Email: [wangwuyou@ycit.edu.cn](mailto:wangwuyou@ycit.edu.cn); [dongpy11@gmail.com](mailto:dongpy11@gmail.com); [xxg@ycit.cn](mailto:xxg@ycit.cn)

## Characterization

The crystal structures of BTO, BVO, and BTO/BVO heterostructures were identified via an X-ray diffractometer (XRD, X'Pert3Powder) with Cu K $\alpha$  irradiation. Raman spectroscopy (LEICA DM 2700 M) was carried out to elucidate the local structure and bonding states from the vibrational spectra. Scanning electron microscopy (SEM) images and EDX-Mapping were carried out on Nova NanoSEM 450 equipped with an energy-dispersive X-ray Spectrometer (AZtec X-MaxN80) to study the surface morphology and element distribution. Transmission electron microscopy (TEM, JEM-1400plus) was used to further explore the micromorphology and lattice planes. X-ray photoelectron spectroscopic (XPS) analysis was performed over an ESCALAB 250Xi spectrometer to manifest elements chemical status. UV–vis diffuse reflection spectroscopy was characterized by a Shimadzu UV–vis 3600 spectrometer to evaluate the optical absorption performance. The separation efficiency of photoexcited carriers was analyzed by steady-state photoluminescence (PL) emission spectra (JASCO FP-6500) and time-resolved PL decay spectra (FL1000). **The light intensity was measured by a power meter (Newport, model: 843-R).** The electron spin resonance (ESR) measurements were depicted on a Bruker ER200-SRC under UV–vis illumination to detect radical  $\bullet\text{O}_2^-$  and radical  $\bullet\text{OH}$ .

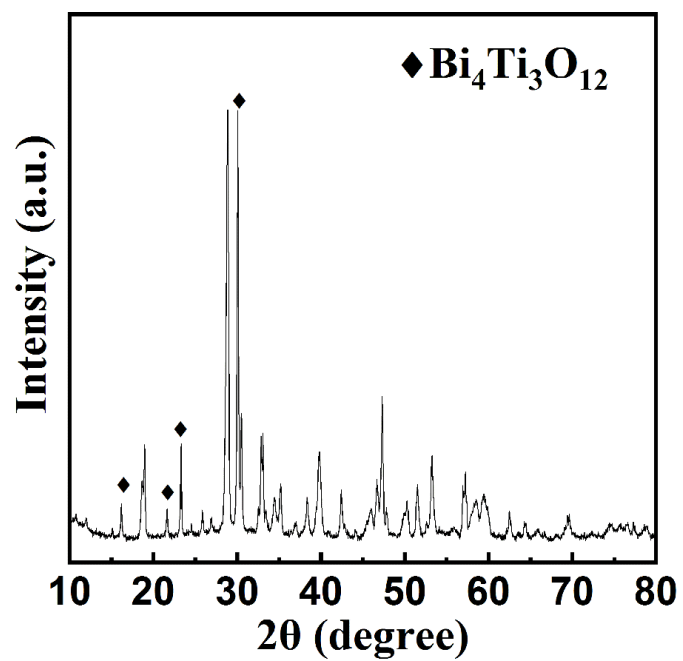


Fig. S1 XRD images of BTO/BVO-20 heterostructures.

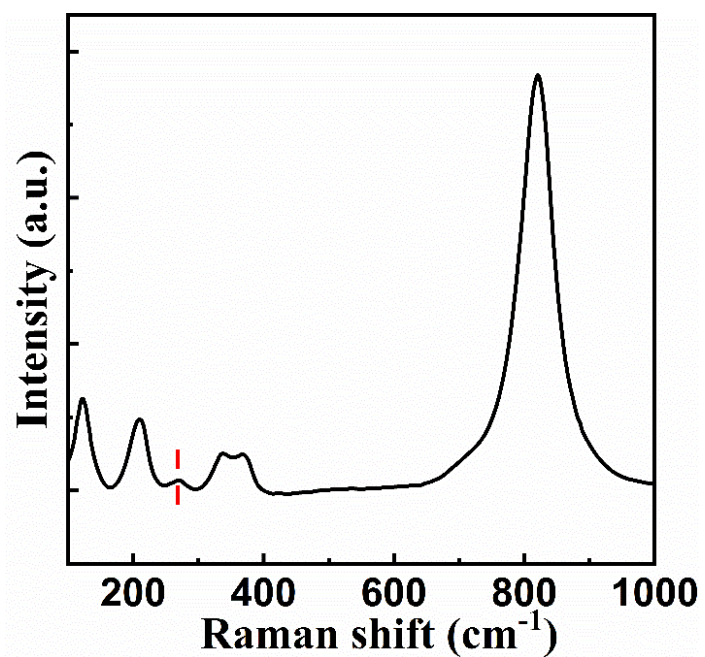
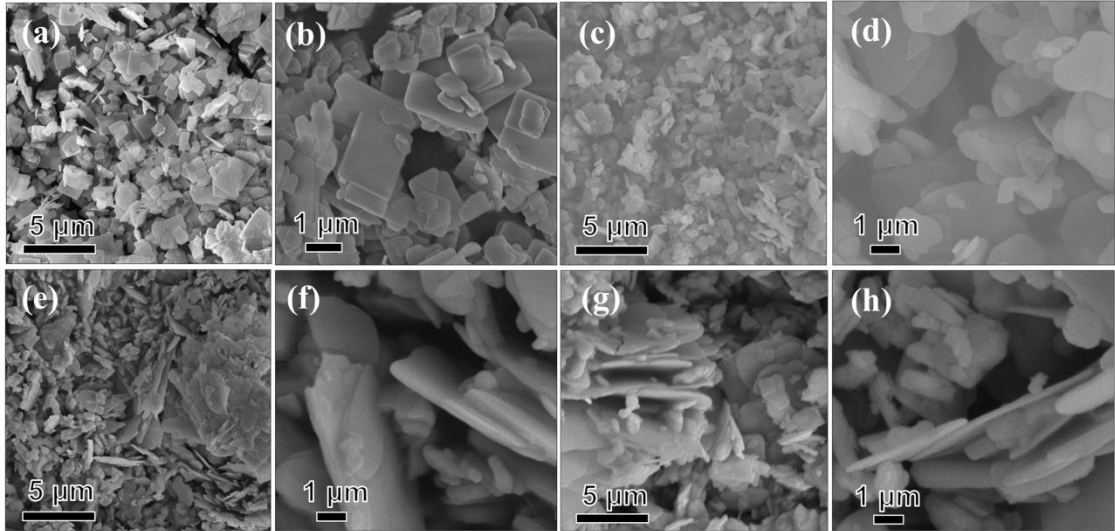
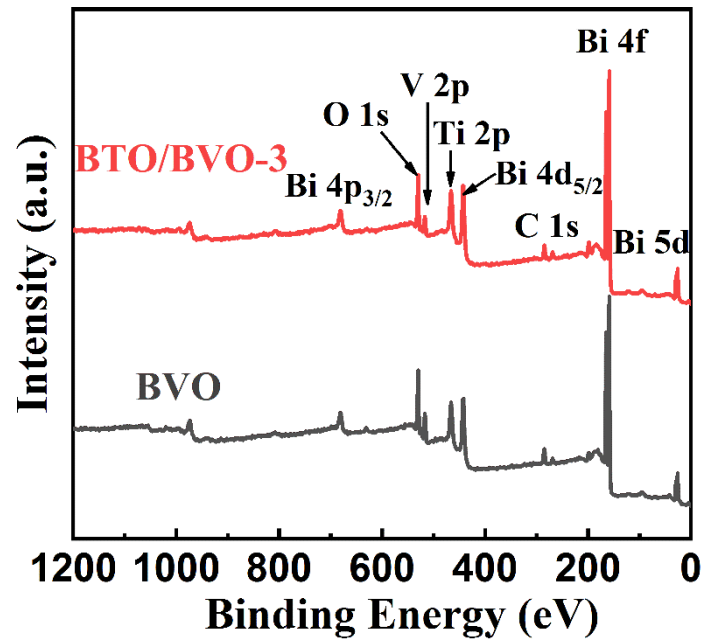


Fig. S2 Raman spectra of BTO/BVO-20 heterostructures.



**Fig. S3** SEM images of samples: (a, b) BTO, (c, d) BVO, (e, f) BTO/BVO-0.5, and (g, h) BTO/BVO-8.



**Fig. S4** XPS survey spectrum of BVO and the BTO/BVO-3 heterostructure.

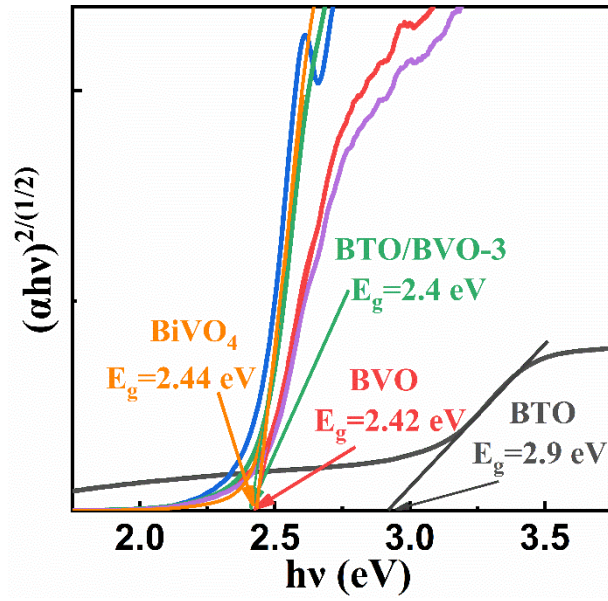


Fig. S5 Tauc plots (b) of BiVO<sub>4</sub>, BVO, BTO, and the BTO/BVO-3 heterostructures.

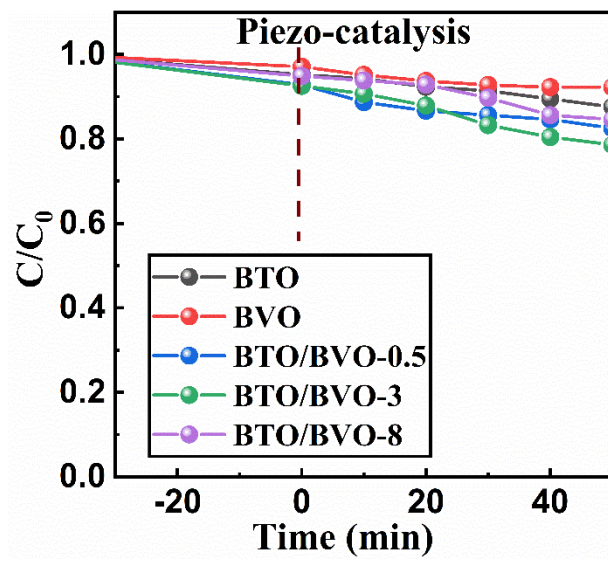
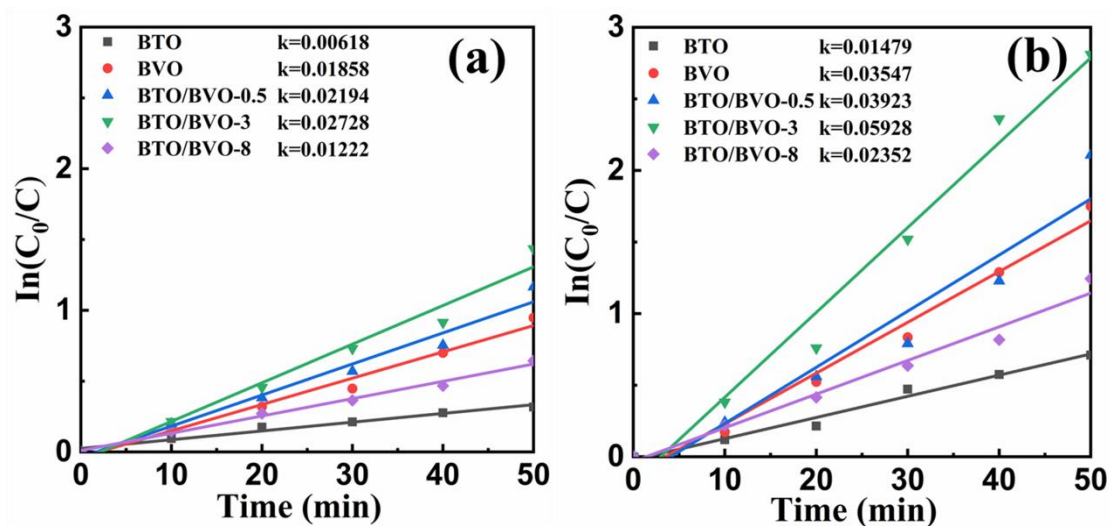
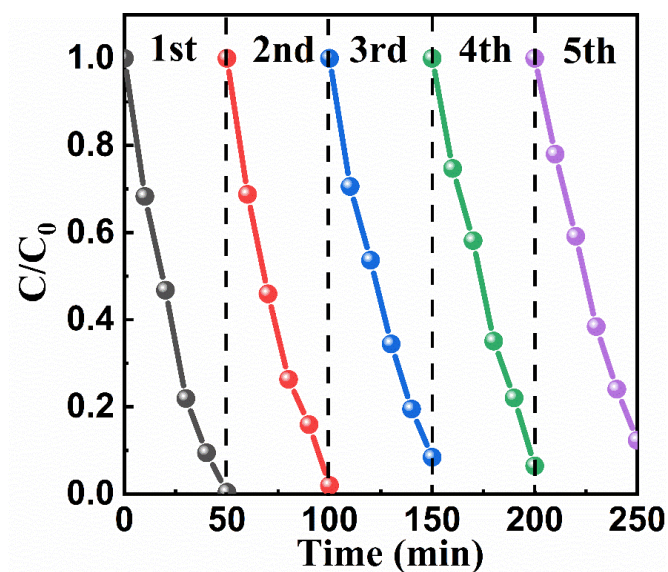


Fig. S6 The removal ratio of Cr(VI) using BTO, BVO, and BTO/BVO heterostructures under piezo-catalysis.



**Fig. S7** The photo-reducing reaction kinetics of Cr(VI) solution: (a) under simulated solar light irradiation and (b) under both ultrasonic vibrations and simulated solar light irradiation using BTO, BVO, and BTO/BVO heterostructures.



**Fig. S8** The cycling performance for piezo-photocatalytic Cr(VI) reduction using the BTO/BVO-3 heterostructure.

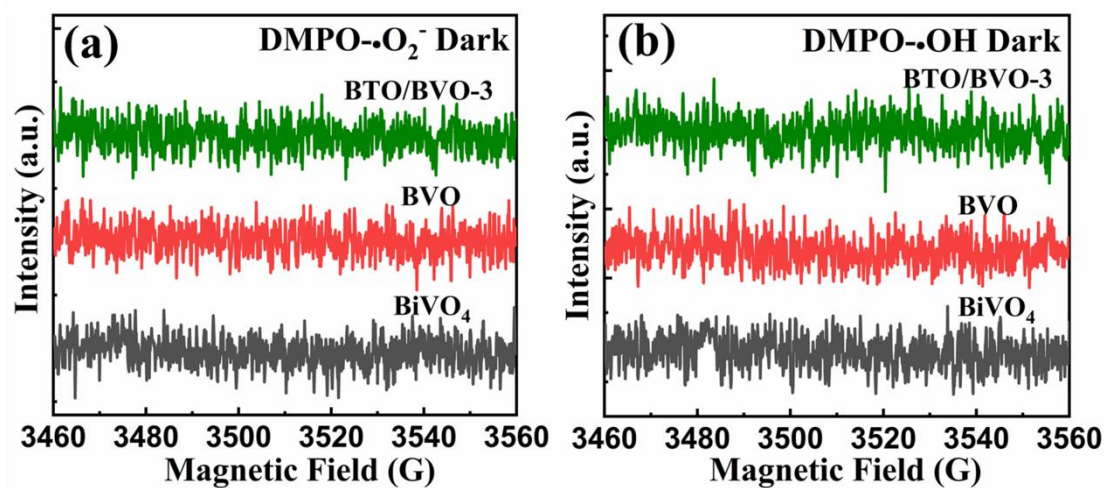


Fig. S9 ESR spectra of (a) DMPO-•O<sub>2</sub><sup>-</sup> and (b) DMPO-•OH signals at dark over BiVO<sub>4</sub>, BVO, and the BTO/BVO-3 heterostructure.